

Neutron Diffraction Study of Magnesium Fluoride Single Crystals

BY GENEVIÈVE VIDAL-VALAT

Laboratoire d'Infra-rouge, Groupe de Dynamique des Phases Condensées (LA 233), USTL, place Eugène Bataillon, 34060 Montpellier CEDEX, France

JEAN-PIERRE VIDAL

Laboratoire de Minéralogie Cristallographie, Groupe de Dynamique des Phases Condensées (LA 233), USTL, place Eugène Bataillon, 34060 Montpellier CEDEX, France

CLAUDE M. E. ZEYEN

Institut Laue–Langevin, 156 X Centre de Tri, 38042 Grenoble CEDEX, France

AND KAARLE KURKI-SUONIO

Department of Physics, University of Helsinki, Siltavuorenpenger 20 D, SF-00170 Helsinki 17, Finland

(Received 5 January 1978; accepted 12 March 1979)

Abstract

Integrated neutron diffraction intensities of MgF_2 single crystals were measured at 300 and 52 K. Refinements of different extinction models were made. A model with mosaic-spread extinction only was found to be most consistent with the data. No evidence was found of its anisotropy. The values of the Mg–F bond length and of the anisotropy parameters $\Delta_1 U = U_z - \bar{U}$ and $\Delta_2 U = (U_{\perp} - U_{\parallel})/2 = -U_{12}$ of the thermal vibrations were independent of the extinction model, while the average isotropic \bar{U} varied considerably. The coordinates of the F^- ion were independent of temperature corresponding to the bond lengths 1.984 (1) and 1.979 (1) Å at 300 and 52 K respectively. Strong anisotropy [with $\Delta_1 U = -0.0017$ (4) and $\Delta_2 U = 0.0034$ (2) Å²] of the vibrations of F^- was observed at 300 K. The results indicate strong excitation of a libration-like mode of the MgF_2 molecule at 300 K but not at 52 K, in accordance with lattice-dynamical considerations.

Introduction

Magnesium fluoride belongs to the tetragonal space group $P4_2/mnm$. Fig. 1 shows the unit cell, where the positions of the ions are:

$$\text{Mg}: (0,0,0); (\frac{1}{2}, \frac{1}{2}, \frac{1}{2}),$$

$$\text{F}: \pm(x, x, 0); (\frac{1}{2}, \frac{1}{2}, \frac{1}{2}) \pm (x, -x, 0),$$

with one structural parameter x defining the Mg–F bond length $d = x\sqrt{2}a$. Since the thermal axes are

defined by symmetry, there are three independent thermal parameters for both Mg and F.

An X-ray diffraction study of MgF_2 by Vidal-Valat (1975) at room temperature yielded the lattice parameters: $a = b = 4.628$ (5), $c = 3.045$ (3) Å, and $x = 0.303$ corresponding to $d = 1.981$ (2) Å.

Direct atomic-charge-density analysis by the method of Kurki-Suonio (1967) indicated some charge transfer from the fluorine towards the magnesium. Distinction between the effects of atomic deformation and of a shift of position could not however be made. Also the observed anisotropy obviously included contributions due to thermal motion and deformation which could not easily be separated from each other. Difficulties of interpretation were partly caused by extinction effects, the presence of which was clearly observed during the X-ray experiments.

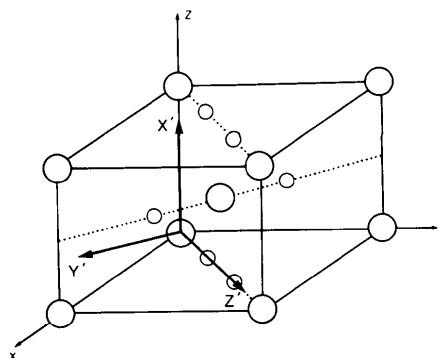


Fig. 1. Unit cell of MgF_2 . XYZ: International Tables for X-ray Crystallography (1969) reference system. X'Y'Z': site symmetry reference system.

To obtain more reliable values for the position of the F^- ion and for the anisotropic thermal parameters independent of the asphericity of atomic-charge distribution, a neutron study was found necessary.

In the present paper we report neutron diffraction measurements at 300 and 52 K and subsequent results obtained by conventional fitting procedures including different possibilities to take extinction effects into account.

Experimental

A large single crystal of MgF_2 was grown in our laboratory (Laboratoire d'Infra-rouge, USTL Montpellier). To study and minimize the effects of extinction, we gave four crystals cut from the large one different quenching treatments. Then, using the γ -ray diffractometer at the Institut Laue-Langevin (Schneider, 1974) we measured the line profiles at a wavelength of $\lambda = 0.03 \text{ \AA}$ from small scattering volumes distributed evenly over the whole samples. This was done for both the 002 and 220 reflections because they displayed the greatest amount of extinction in the X-ray study. Those parts of the crystals which showed a peak width less than the horizontal neutron beam divergence were selected. Two rectangular parallelepipeds of 12.7 and 4 mm^3 were cut from them and used as the samples in the ordinary neutron diffraction study.

Neutron data collection was carried out at 300 and 52 K at the High Flux Reactor of the Institut Laue-Langevin using the D9 four-circle diffractometer at a wavelength of 0.5894 \AA .

The low-temperature data were collected using a closed-loop single-stage Displex refrigerator cryostat. The temperature was monitored using an Au 0.07 Fe/Cr thermocouple and kept constant to within $\pm 2 \text{ K}$.

At room temperature, exactly the same lattice parameters as in the X-ray experiment were found. At 52 K these parameters were: $a = b = 4.615 (5)$, $c = 3.043 (3) \text{ \AA}$.

The full ω , $X\theta$ step-scan mode (30 points per scan) (Werner, 1971) was used at a rate of about 4 min per reflection.

The scan parameter X was determined experimentally as a function of the Bragg angle using our samples. Two standard reflections measured after every 30 reflections gave a combined standard deviation of the source and counting chain of less than 1%. The integrated intensities of 328 reflections were measured from the larger sample to obtain a set of non-equivalent structure factors which was as complete as possible up to $\sin \theta/\lambda = 0.97 \text{ \AA}^{-1}$.

Reflections with irregular profiles were discarded. As a check, the 35 most extinguished reflections were remeasured at both 300 and 52 K on the small crystal under the same experimental conditions except that a

longer counting time was used. Only volume-corrected intensities displaying improved extinction conditions were considered in the subsequent analysis.

Renninger scans were run for the 002 reflection to test for the possible existence of multiple scattering. No significant effect was detected.

Analysis of data

Lorentz, background and counter dead time corrections were applied to the observed intensities. The background was calculated using the method of Lehmann & Larsen (1974). Effective path-length values were computed for all reflections for both samples to correct for absorption and extinction effects. Absorption corrections were estimated to be of the order of 0.1% at most, so no corrections were applied.

Anisotropic thermal diffuse scattering corrections were computed using the method of de With, Harkema & Feils (1976) and the elastic constants of Aleksandrov, Shabanova & Zinenko (1969). Since the method is intended for $\omega/2\theta$ scans we approximated our scan parameter by a step function and used corresponding constant values of X in the calculation. The corrections obtained were extremely small, of the order of 0.01% in F_{hkl} at most, and thus negligible. The approximation made is therefore of no significance.

For the refinement, the latest version of the *LINEX* program of Becker & Coppens (1975) was adopted. It allows the treatment of extinction in terms of a variety of different models together with the bond lengths, thermal parameters and the scale factor. To study the extinction in MgF_2 several models were applied. Isotropic as well as anisotropic extinction with secondary extinction of mosaic-spread type (type I) or particle-size type (type II) without and together with primary extinction were tested. The nuclear scattering amplitudes were those of Bacon (1977) and were not refined during the analysis. The main refinements were based on F_{hkl} and consisted of the following models.

In the models (1*i*), (2*i*), (3*i*) both thermal motion and extinction are isotropic. In (1*i*) the extinction is of type I characterized by the mosaic-spread parameter g . Model (2*i*) allows only type II extinction with the particle-size parameter r . Model (3*i*) contains both parameters g for type I and r for type II and primary extinction.

Models (1), (2) and (3) differ from (1*i*), (2*i*) and (3*i*) only in their anisotropic thermal motion. All six thermal parameters allowed by symmetry are varied.

In the models (1*a*) to (4*a*) both thermal motion and extinction are anisotropic. The type I extinction of model (1*a*) is described by the mosaic-spread tensor (g_{ij}) with two independent components $g_{11} = g_{22}$ and g_{33} only, due to symmetry. The type II or particle-size extinction of model (2*a*) is similarly represented by the tensor (E_{ij}) with two variable parameters $E_{11} = E_{22}$ and

E_{33} . Model (3a) contains the extinction model of Thornley & Nelmes (1974). It uses the more general formalism with both types of secondary and primary extinction. The mosaic spread related to the type I extinction is described by a tensor \mathbf{Y} directly proportional to the mosaic spread. The type II and primary extinction are isotropic and described with the particle-size parameter r .

In model (4a) the extinction model of Coppens & Hamilton (1970) is used. The same types of extinction as in model (3a) are taken into account. However, the mosaic-spread tensor \mathbf{Z} is now inversely proportional to the mosaic spread.

Tables 1 and 2 report the isotropic results obtained from the 300 and 52 K measurements respectively. For refinement of the isotropic models (1i) and (3i) the initial value of the mosaic-spread parameter g was determined experimentally. It was deduced from the half width of 0.5' of arc from the γ -ray profile of the most extinguished reflection 002.

Tables 3 and 4 give the results for models (1), (2) and (3) and Tables 5 and 6 give those for the anisotropic models. The results of (3a) and (4a) were obtained using a Gaussian mosaic-spread distribution in the treatment of type I extinction. Calculations with a Lorentzian distribution always gave larger R values and were therefore discarded. The values of the components of the mosaic-spread tensor (\mathbf{Y} or \mathbf{Z}) were

initialized from the isotropic mosaic spread g of the model (3i).

Tables 1 to 6 list vertically the reliability factor R , the weighted factor R_w , the parameter x , the mean-square vibration amplitudes U_i (or U_{ij}) in \AA^2 , the extinction parameters, the scale factor and the lowest extinction coefficients y . The final structure factors corresponding to a double unit cell, their standard deviations and extinction coefficients are reported in Tables 7 and 8.

Discussion

On the basis of the results given in Tables 1 to 6 some conclusions can be drawn on the applicability of the different extinction models to our samples. Type I extinction yields systematically slightly lower R factors

Table 1. *Isotropic least-squares refined parameters of MgF_2 at 300 K*

	Model (1i) variable g	Model (3i) variables g and r	Model (2i) variable r
R	0.024	0.024	0.024
R_w	0.030	0.029	0.030
x	0.3031 (3)	0.3030 (3)	0.3030 (3)
$\text{Mg}^{2+} U_i (\text{\AA}^2)$	0.0044 (3)	0.0040 (4)	0.0029 (3)
$\text{F}^- U_i (\text{\AA}^2)$	0.0078 (3)	0.0075 (3)	0.0065 (3)
$g (\times 10^4)$	0.79 (7)	0.6 (1)	
$r/\lambda (\times 10^4)$		12 (3)	1.6 (2)
Scale factor	7.5 (1)	7.5 (1)	7.3 (1)
Lowest y	0.48	0.50	0.58

Table 2. *Isotropic least-squares refined parameters of MgF_2 at 52 K*

	Model (1i) variable g	Model (3i) variables g and r	Model (2i) variable r
R	0.013	0.013	0.015
R_w	0.017	0.017	0.019
x	0.3030 (2)	0.3030 (2)	0.3030 (2)
$\text{Mg}^{2+} U_i (\text{\AA}^2)$	0.0021 (2)	0.0018 (2)	0.0004 (2)
$\text{F}^- U_i (\text{\AA}^2)$	0.0037 (2)	0.0034 (2)	0.0022 (2)
$g (\times 10^4)$	0.72 (4)	0.6 (1)	
$r/\lambda (\times 10^4)$		9 (2)	1.3 (8)
Scale factor	7.45 (7)	7.40 (7)	7.12 (6)
Lowest y	0.48	0.50	0.61

Table 3. *Least-squares refined parameters of MgF_2 at 300 K (isotropic extinction–anisotropic thermal motion)*

	Model (1) variable g (Type I)	Model (3) g and r (Types I, II, P)	Model (2) variable r (Type II)
R	0.010	0.010	0.012
R_w	0.014	0.013	0.015
x	0.3032 (2)	0.3032 (1)	0.3031 (2)
$\text{Mg}^{2+} \begin{cases} U_{11} = U_{22} (\text{\AA}^2) \\ U_{33} (\text{\AA}^2) \\ U_{12} (\text{\AA}^2) \end{cases}$	$\begin{cases} 0.0053 (3) \\ 0.0036 (3) \\ -0.0004 (2) \end{cases}$	$\begin{cases} 0.0050 (3) \\ 0.0033 (3) \\ -0.0005 (2) \end{cases}$	$\begin{cases} 0.0038 (3) \\ 0.0023 (3) \\ -0.0006 (2) \end{cases}$
$\text{F}^- \begin{cases} U_{11} = U_{22} (\text{\AA}^2) \\ U_{33} (\text{\AA}^2) \\ U_{12} (\text{\AA}^2) \end{cases}$	$\begin{cases} 0.0087 (2) \\ 0.0062 (2) \\ -0.0034 (2) \end{cases}$	$\begin{cases} 0.0084 (2) \\ 0.0058 (2) \\ -0.0033 (2) \end{cases}$	$\begin{cases} 0.074 (3) \\ 0.0048 (2) \\ -0.0033 (2) \end{cases}$
$g (\times 10^4)$	0.78 (3)	0.58 (6)	
$r/\lambda (\times 10^4)$		12 (1)	1.59 (8)
Scale factor	7.50 (5)	7.46 (5)	7.25 (6)
Lowest y	0.47	0.49	0.58

Table 4. *Least-squares refined parameters of MgF_2 at 52 K (isotropic extinction–anisotropic thermal motion)*

	Model (1) variable g (Type I)	Model (3) g and r (Types I, II, P)	Model (2) variable r (Type II)
R	0.012	0.012	0.013
R_w	0.016	0.016	0.018
x	0.3031 (2)	0.3030 (2)	0.3030 (2)
$\text{Mg}^{2+} \begin{cases} U_{11} = U_{22} (\text{\AA}^2) \\ U_{33} (\text{\AA}^2) \\ U_{12} (\text{\AA}^2) \end{cases}$	$\begin{cases} 0.0023 (3) \\ 0.0020 (3) \\ 0.0003 (2) \end{cases}$	$\begin{cases} 0.0020 (4) \\ 0.0016 (4) \\ 0.0003 (3) \end{cases}$	$\begin{cases} 0.0006 (4) \\ 0.0004 (4) \\ 0.0001 (3) \end{cases}$
$\text{F}^- \begin{cases} U_{11} = U_{22} (\text{\AA}^2) \\ U_{33} (\text{\AA}^2) \\ U_{12} (\text{\AA}^2) \end{cases}$	$\begin{cases} 0.0041 (2) \\ 0.0030 (2) \\ -0.0005 (2) \end{cases}$	$\begin{cases} 0.0038 (3) \\ 0.0026 (3) \\ -0.0005 (2) \end{cases}$	$\begin{cases} 0.0026 (3) \\ 0.0014 (3) \\ -0.0004 (2) \end{cases}$
$g (\times 10^4)$	0.72 (4)	0.58 (8)	
$r/\lambda (\times 10^4)$		9 (2)	1.32 (8)
Scale factor	7.46 (7)	7.41 (7)	7.13 (6)
Lowest y	0.48	0.50	0.61

Table 5. *Least-squares refined parameters of MgF₂ at 300 K (anisotropic extinction and thermal motion)*

	Model (1a)	Model (2a)	Model (3a) (Thornley & Nelmes, 1974)	Model (4a) (Coppens & Hamilton, 1970)
R	0.010	0.011	0.010	0.010
R_w	0.014	0.016	0.013	0.013
x	0.3032 (1)	0.3031 (1)	0.3032 (1)	0.3032 (1)
Mg^{2+} $\begin{cases} U_{11} = U_{22} (\text{Å}^2) \\ U_{33} (\text{Å}^2) \\ U_{12} (\text{Å}^2) \end{cases}$	$\begin{cases} 0.0053 (3) \\ 0.0036 (3) \\ -0.0004 (2) \end{cases}$	$\begin{cases} 0.0038 (3) \\ 0.0020 (3) \\ -0.0005 (2) \end{cases}$	$\begin{cases} 0.0050 (3) \\ 0.0033 (3) \\ -0.0005 (2) \end{cases}$	$\begin{cases} 0.0049 (3) \\ 0.0033 (3) \\ -0.0005 (2) \end{cases}$
F^- $\begin{cases} U_{11} = U_{22} (\text{Å}^2) \\ U_{33} (\text{Å}^2) \\ U_{12} (\text{Å}^2) \end{cases}$	$\begin{cases} 0.0087 (2) \\ 0.0062 (2) \\ -0.0034 (2) \end{cases}$	$\begin{cases} 0.0074 (2) \\ 0.0045 (2) \\ -0.0033 (2) \end{cases}$	$\begin{cases} 0.0084 (2) \\ 0.0060 (2) \\ -0.0033 (2) \end{cases}$	$\begin{cases} 0.0084 (2) \\ 0.0059 (2) \\ -0.0033 (2) \end{cases}$
	$(g_{11} = g_{22}) \times 10^4 = 1.6 (2)$ $g_{33} \times 10^4 = 1.6 (2)$	$(E_{11} = E_{22}) \times 10^4 = 0.63 (9)$ $E_{33} \times 10^4 = 0.1 (3)$	$(Y_{11} = Y_{22}) \times 10^4 = 2.9 (8)$ $Y_{33} \times 10^4 = 2.7 (6)$	$(Z_{11} = Z_{22}) \times 10^{-4} = 0.33 (9)$ $Z_{33} \times 10^{-4} = 0.36 (9)$
$r/\lambda (\times 10^4)$			11 (2)	11 (2)
Scale factor	7.50 (6)	7.21 (5)	7.45 (5)	7.47 (6)
Lowest y	0.49	0.63	0.50	0.50

Table 6. *Least-squares refined parameters of MgF₂ at 52 K (anisotropic extinction and thermal motion)*

	Model (1a)	Model (2a)	Model (3a) (Thornley & Nelmes, 1974)	Model (4a) (Coppens & Hamilton, 1970)
R	0.012	0.013	0.012	0.012
R_w	0.016	0.018	0.016	0.016
x	0.3031 (2)	0.3030 (2)	0.3030 (2)	0.3030 (2)
Mg^{2+} $\begin{cases} U_{11} = U_{22} (\text{Å}^2) \\ U_{33} (\text{Å}^2) \\ U_{12} (\text{Å}^2) \end{cases}$	$\begin{cases} 0.0023 (3) \\ 0.0019 (4) \\ 0.0003 (2) \end{cases}$	$\begin{cases} 0.0006 (4) \\ 0.0002 (4) \\ 0.0002 (3) \end{cases}$	$\begin{cases} 0.0020 (4) \\ 0.0016 (4) \\ 0.0003 (2) \end{cases}$	$\begin{cases} 0.0020 (4) \\ 0.0016 (4) \\ 0.0003 (2) \end{cases}$
F^- $\begin{cases} U_{11} = U_{22} (\text{Å}^2) \\ U_{33} (\text{Å}^2) \\ U_{12} (\text{Å}^2) \end{cases}$	$\begin{cases} 0.0041 (2) \\ 0.0029 (3) \\ -0.0005 (2) \end{cases}$	$\begin{cases} 0.0026 (3) \\ 0.0012 (3) \\ -0.0004 (2) \end{cases}$	$\begin{cases} 0.0038 (3) \\ 0.0026 (3) \\ -0.0005 (2) \end{cases}$	$\begin{cases} 0.0038 (3) \\ 0.0026 (3) \\ -0.0005 (2) \end{cases}$
	$(g_{11} = g_{22}) \times 10^4 = 1.9 (3)$ $g_{33} \times 10^4 = 1.9 (3)$	$(E_{11} = E_{22}) \times 10^4 = 0.8 (1)$ $E_{33} \times 10^4 = 0.2 (4)$	$(Y_{11} = Y_{22}) \times 10^4 = 2.7 (8)$ $Y_{33} \times 10^4 = 2.7 (8)$	$(Z_{11} = Z_{22}) \times 10^{-4} = 0.3 (1)$ $Z_{33} \times 10^{-4} = 0.3 (1)$
$r/\lambda (\times 10^4)$			8 (3)	9 (2)
Scale factor	7.46 (7)	7.11 (6)	7.42 (7)	7.41 (7)
Lowest y	0.49	0.64	0.51	0.51

than type II. Further improvement obtained by including both types plus primary extinction is insignificant.

The improvement of fit produced by the thermal anisotropy is very noticeable at room temperature but only marginal at 52 K. The anisotropy of extinction, however, has no effect at all. It is thus concluded that the extinction is isotropic within the experimental accuracy and that the type I or the mosaic-spread extinction model corresponds somewhat more closely to the true phenomenon in our samples.

Inclusion of the particle-size parameter r systematically lowers the values of the thermal parameters, even leading to quite unrealistic results. The inadequacy of type II extinction is obvious also from the ratio $\bar{U}_F/\bar{U}_{\text{Mg}}$, which in the case of model (1) has the value 1.68 at both temperatures, and 1.70 and 1.72 at 300 and 52 K respectively for model (3). These are both reasonably close to the square mass ratio $(\text{Mg}/\text{F})^2 = 1.64$ as would be expected. For model (2) values of 2.0 and 4.0 are obtained for the ratio at 300 and 52 K, respectively, which seem quite unrealistic.

Because of this unfavourable coupling of the parameter r to the temperature factors we regard the

parameters of model (1) with isotropic mosaic-spread extinction only as the ordinary results of our analysis. However, we do not think that the reliability of the parameters obtained should be deduced on the basis of the best model alone, but the variations of their values as the model is varied should also be considered. In particular, it is doubtful if any physical sense can be attributed to the values of the extinction parameters themselves, obtained in the refinement.

The value of x is independent of the model applied. We can therefore attach a high reliability to the value $x = 0.3032 (2)$ obtained, corresponding to the Mg—F bond lengths of 1.984 (1) and 1.979 (1) Å at 300 and 52 K respectively.

In order to discuss the physical nature and reliability of the results concerning thermal motion, in Table 9 several parameters for the different models are listed. First we refer to the principal-axis representation $U_x S_x^2 + U_y S_y^2 + U_z S_z^2$ of the thermal quadratic form where S_x , S_y and S_z are the components of the scattering vector and give the principal mean-square amplitudes $U_x = U_{\parallel} = U_{11} + U_{12}$ along the bond direction, $U_y = U_{\perp} = U_{11} - U_{12}$ perpendicular to the bond direction in the xy plane and $U_z = U_{33}$ along the z axis.

Table 7. *Experimental and calculated structure factors of MgF₂ with relative deviations and extinction parameters on F₀ at 300 K (model 1)*

H	K	L	F ₀	F _c	σF/F ₀	γ	H	K	L	F	F _c	σF/F ₀	γ	H	K	L	F ₀	F _c	σF/F ₀	γ
1	1	0	2.588	2.510	0.006	0.72	4	4	1	-3.241	-3.218	0.008	0.86	4	2	4	1.220	1.198	0.021	0.98
1	0	1	0.540	0.614	0.025	0.98	5	1	2	2.935	2.915	0.008	0.88	6	1	3	1.303	1.305	0.020	0.97
2	0	0	-1.290	-1.365	0.009	0.92	6	0	0	3.051	3.162	0.008	0.86	7	3	0	3.376	3.428	0.020	0.86
1	1	1	-2.182	-2.178	0.005	0.81	5	3	1	5.111	5.111	0.005	0.70	5	5	2	4.519	4.533	0.007	0.81
2	1	0	2.273	2.339	0.006	0.75	6	1	0	5.176	5.467	0.005	0.70	7	1	2	4.519	4.533	0.007	0.81
2	2	0	*5.83	*5.88	0.005	0.61	4	1	3	2.801	2.849	0.009	0.88	1	1	5	-2.833	-2.826	0.009	0.91
0	0	2	6.303	6.266	0.004	0.47	4	2	3	1.435	1.443	0.016	0.97	7	3	1	1.340	1.296	0.019	0.97
3	1	0					5	2	3					6	2	3	-1.750	-1.687	0.015	0.96
2	2	1	-1.541	-1.525	0.011	0.94	3	3	3	-0.886	-0.849	0.027	0.99	6	5	0				
1	1	2	2.505	2.424	0.008	0.87	1	1	4	2.203	2.186	0.011	0.93	6	4	2	2.210	2.213	0.012	0.94
3	0	1	5.417	5.444	0.005	0.54	6	1	1	1.111	1.372	0.017	0.97	5	4	3	0.992	0.958	0.027	0.98
3	1	1	2.095	2.057	0.009	0.90	6	2	0					4	3	4	1.631	1.617	0.016	0.97
3	2	0	-1.465	-1.438	0.012	0.95	2	0	4	-2.058	-2.028	0.012	0.94	7	2	2				
2	0	2	-1.119	-1.252	0.016	0.96	5	4	0					2	1	5	2.500	2.494	0.011	0.93
2	1	2	2.460	2.407	0.009	0.88	4	2	3	2.058	2.028	0.012	0.94	5	1	4	2.629	2.591	0.010	0.92
3	2	1	-0.629	-0.751	0.009	0.98	4	4	2	1.634	1.592	0.015	0.96	8	1	4				
2	4	0	2.770	2.836	0.008	0.84	2	1	4	-1.890	-1.875	0.013	0.95	8	0	0				
4	1	0	-3.481	-3.597	0.007	0.77	5	3	2	-1.085	-1.037	0.022	0.98	8	1	0	-1.081	-1.088	0.024	0.98
2	2	2	*0.689	*0.357	0.006	0.72	5	4	1	1.023	0.989	0.024	0.98	7	4	0	-1.084	-1.173	0.015	0.96
3	3	0	*0.795	*0.005	0.009	0.69	2	2	4	3.902	3.832	0.007	0.84	2	2	5	-1.177	-1.116	0.022	0.98
3	1	2	0.915	0.872	0.022	0.98	6	3	0	-1.390	-1.388	0.018	0.97	6	3	3	2.474	2.440	0.010	0.93
4	1	1	1.495	1.518	0.014	0.95	6	0	2	3.054	3.036	0.008	0.88	3	0	5	4.115	4.171	0.007	0.83
4	2	0	1.329	1.307	0.015	0.96	5	0	3	2.533	2.483	0.010	0.92	5	2	4				
3	3	1	-0.923	-0.944	0.022	0.98	5	0	3	-1.558	-1.525	0.016	0.96	7	3	2	3.263	3.285	0.008	0.88
1	0	3	0.664	0.636	0.054	0.99	6	1	2	2.702	2.703	0.009	0.90	7	4	1	2.225	2.219	0.011	0.94
3	2	2	-1.346	-1.364	0.015	0.96	5	1	3					3	1	5	1.505	1.500	0.016	0.97
4	2	1	2.218	2.253	0.010	0.91	3	1	4	0.868	0.856	0.029	0.99	8	2	0	3.405	3.399	0.008	0.87
1	1	3	-3.515	-3.400	0.007	0.82	6	3	1	2.592	2.592	0.010	0.91	8	2	0	1.824	1.859	0.017	0.97
4	3	0	1.953	1.995	0.011	0.83	5	2	3	*1.157	*1.142	0.007	0.81	7	0	3	3.425	3.461	0.007	0.88
4	0	2	2.732	2.731	0.008	0.88	5	2	3					6	5	2				
2	1	3	2.914	2.906	0.008	0.87	7	1	0					8	2	1	-1.747	-1.776	0.013	0.96
5	1	0	2.894	3.032	0.009	0.85	3	2	4	-1.181	-1.164	0.022	0.98	8	2	1				
3	3	2	-3.142	-3.121	0.007	0.82	5	5	0	*0.511	*0.637	0.006	0.78	3	2	4				
3	3	2	*0.575	*4.408	0.006	0.75	5	0	0					5	3	3				
4	3	1	2.729	2.677	0.008	0.89	7	0	1	3.739	3.773	0.007	0.83	5	3	3				
5	0	1	-1.776	-1.776	0.013	0.94	6	4	0	2.285	2.297	0.011	0.93	5	3	4				
5	2	3					7	1	1	-1.986	-1.974	0.012	0.95	6	6	0				
5	2	0	-1.385	-1.372	0.016	0.97	5	1	1					6	0	4	2.442	2.410	0.009	0.93
4	2	2	1.201	1.279	0.018	0.97	4	4	3	-2.931	-2.895	0.009	0.90	6	0	4	2.645	2.690	0.008	0.92
3	3	3	*0.759	*0.759	0.009	0.70	4	0	4	2.385	2.440	0.011	0.92	8	3	0				
3	1	3	1.880	1.852	0.012	0.94	7	2	0	1.123	1.143	0.023	0.98	8	0	2				
5	2	1	*0.514	*0.522	0.009	0.80	6	1	4	-2.944	-2.913	0.008	0.90	8	0	2				
4	4	0	1.636	1.638	0.013	0.95	6	3	2	-1.356	-1.316	0.019	0.97	7	1	4	2.279	2.308	0.010	0.94
5	3	0	-0.589	-0.589	0.008	0.89	6	4	1	2.740	2.677	0.010	0.91	7	5	0				
5	3	0	-1.123	-1.132	0.021	0.98	5	3	3					6	4	2	-1.626	-1.634	0.013	0.97
4	3	2	1.892	1.893	0.012	0.94	3	3	1	3.913	3.871	0.007	0.85	6	6	1	-1.996	-1.959	0.011	0.95

* Unobserved reflections.

Table 8. *Experimental and calculated structure factors of MgF₂ with relative deviations and extinction parameters on F₀ at 52 K (model 1)*

H	K	L	F ₀	F _c	σF/F ₀	γ	H	K	L	F ₀	F _c	σF/F ₀	γ	H	K	L	F ₀	F _c	σF/F ₀	γ
1	1	0	2.542	2.543	0.005	0.73	4	4	1	-3.740	-3.745	0.007	0.83	4	2	4	1.271	1.188	0.021	0.98
1	0	1	0.501	0.615	0.023	0.98	5	1	2	3.204	3.228	0.008	0.86	6	1	3	1.188	1.368	0.022	0.97
2	0	0	-1.361	-1.405	0.009	0.92	6	0	0	3.425	3.557	0.007	0.84	7	3	0	3.957	*0.958	0.007	0.83
1	1	1	-2.294	-2.390	0.004	0.62	5	3	1	5.995	5.995	0.005	0.67	5	5	2	5.513	5.426	0.005	0.75
2	1	0	2.483	2.569	0.006	0.80	6	1	0	5.785	5.995	0.005	0.67	7	1	2				
2	1	1	3.285	3.178	0.006	0.76	6	1	0	3.218	3.337	0.008	0.86	1	1	5	-3.366	-3.392	0.008	0.89
2	2	0	5.170	*7.22	0.004	0.68	4	1	3	1.678	1.612	0.015	0.96	1	1	5	1.200	1.357	0.022	0.97
0	0	2	6.240	6.413	0.005	0.48	5	2	2					6	2	3	-2.112	-2.075	0.012	0.95
3	1	0					5	2	2	-1.180	-1.139	0.025	0.98	6	5	0				
2	2	1	-1.647	-1.647	0.011	0.93	1	1	4	2.379	2.363	0.011	0.93	6	5	0				
1	1	2	2.550	2.497	0.008	0.87	6	1	1	1.406	1.406	0.018	0.97	6	4	2	2.328	2.258	0.011	0.94
3	0	1	5.593	5.654	0.005	0.59	6	2	0					5	4	3	1.854	1.930	0.013	0.96
3	1	1	2.167	2.180	0.009	0.89	4	2	3	2.367	2.345	0.011	0.93	4	3	4	1.854	1.930	0.013	0.96
3	2	0	-1.437	-1.449	0.013	0.95	2	0	4	-1.201	-1.206	0.024	0.98	7	2	2				
2	0	2	-1.325	-1.353	0.016	0.95	5	4	0					2	1	5	2.815	2.823	0.009	0.91
2	1	2	2.411	2.505	0.008	0.88	4	4	2	2.039	2.067	0.012	0.94	5	1	4	3.018	3.039	0.009	0.90
3	2	1	2.807	2.807	0.008	0.88	2	1	4	2.356	2.322	0.011	0.93	8	2	5	-2.374	-2.373	0.010	0.93
4	0	0	-0.856	-0.796	0.008	0.88	6	2	1	-2.144	-2.182	0.011	0.93	8	0	0				
4	1	0	2.898	3.001	0.007	0.83	5	3	2	-1.146	-1.319	0.020	0.97	8	1	0	-1.553	-1.514	0.016	0.97
4	1	0	-3.827	-3.866	0.006	0.75	5	4	1	1.056	1.014	0.025	0.98	7	4	0	-2.374	-2.373	0.010	0.93
2	2	2	*0.828	*0.828	0.005	0.71	2	2	4	*0.396	*0.333	0.006	0.61	7	5	0	-1.430	-1.446	0.018	0.97
5	3	0	5.013	*0.957	0.005	0.67	6	3	0	-1.076	-1.054	0.012	0.95	6	3	3	3.080	3.043	0.008	0.90
3	1	2	0.763	0.850	0.030	0.98	6	3	0	3.495	3.485	0.007	0.86	3	0	5	*0.819	*0.951	0.006	0.78
4	1	1	1.682	1.662	0.012	0.94	6	0	2	2.864	2.885	0.008	0.91	5	2	4				
4	2	0	1.241	1.246	0.017	0.97	5	0	3	-1.563	-1.495	0.013	0.95	5	3	4				
3	3	1	-1.150	-1.198	0.019															

Table 9. Principal mean-square amplitudes (\AA^2) of MgF_2 at 300 and 52 K

								Niederauer & Gottlicher (1970) (X-ray)	Baur & Khan (1971) (X-ray)	Galtier (1978)	
300 K		Model (1)	Model (3)	Model (2)	Model (1a)	Model (2a)	Model (3a)	Model (4a)			
Mg^{2+}	U_{\parallel}	0.0049 (5)	0.0045	0.0032	0.0049	0.0033	0.0045	0.0044	0.0079	0.0060	
	U_{\perp}	0.0057 (5)	0.0055	0.0044	0.0057	0.0043	0.0055	0.0054	0.0091	0.0071	
	$U_z = U_{33}$	0.0036 (3)	0.0033	0.0023	0.0036	0.0020	0.0033	0.0033	0.0077	0.0046	
	\bar{U}	0.0047 (3)	0.0044	0.0033	0.0047	0.0032	0.0044	0.0044	0.0082	0.0059	
	$U_z - \bar{U}$	-0.0011 (6)	-0.0011	-0.0010	-0.0011	-0.0012	-0.0011	-0.0011	-0.0011	-0.0005	-0.0013
F^-	$\frac{1}{2}(U_{\parallel} - U_{\perp}) = -U_{12}$	0.0004 (2)	0.0005	0.0006	0.0004	0.0005	0.0005	0.0005	0.0006	0.0006	
	U_{\parallel}	0.0053 (4)	0.0051	0.0041	0.0053	0.0041	0.0051	0.0051	0.0102	0.0056	
	U_{\perp}	0.0121 (4)	0.0117	0.0107	0.0121	0.0107	0.0117	0.0117	0.0158	0.0124	
	$U_z = U_{33}$	0.0062 (2)	0.0058	0.0048	0.0062	0.0045	0.0060	0.0059	0.0110	0.0068	
	\bar{U}	0.0079 (2)	0.0075	0.0065	0.0079	0.0064	0.0076	0.0076	0.0123	0.0083	
x	$U_z - \bar{U}$	-0.0017 (4)	-0.0017	-0.0017	-0.0017	-0.0019	-0.0016	-0.0017	-0.0013	-0.0015	
	$\frac{1}{2}(U_{\parallel} - U_{\perp}) = -U_{12}$	0.0034 (2)	0.0033	0.0033	0.0034	0.0033	0.0033	0.0033	0.0028	0.0034	
	x	0.3032 (2)	0.3032 (1)	0.3031 (2)	0.3032 (1)	0.3031 (1)	0.3032 (1)	0.3032 (1)			
	52 K										
	Mg^{2+}	U_{\parallel}	0.0026 (5)	0.0023	0.0007	0.0026	0.0008	0.0023	0.0023		0.0027
U_{\perp}		0.0020 (5)	0.0017	0.0005	0.0020	0.0004	0.0017	0.0017		0.0024	
$U_z = U_{33}$		0.0020 (3)	0.0016	0.0004	0.0019	0.0002	0.0016	0.0016		0.0023	
\bar{U}		0.0022 (3)	0.0019	0.0005	0.0022	0.0005	0.0019	0.0019		0.0027	
$U_z - \bar{U}$		-0.0002 (6)	-0.0003	-0.0001	-0.0003	-0.0003	-0.0003	-0.0003		-0.0004	
F^-	$\frac{1}{2}(U_{\parallel} - U_{\perp}) = -U_{12}$	-0.0003 (2)	-0.0003	-0.0001	-0.0003	-0.0002	-0.0003	-0.0003		0.0002	
	U_{\parallel}	0.0036 (4)	0.0033	0.0022	0.0036	0.0022	0.0033	0.0033		0.0028	
	U_{\perp}	0.0046 (4)	0.0043	0.0030	0.0046	0.0030	0.0043	0.0043		0.0048	
	$U_z = U_{33}$	0.0030 (2)	0.0026	0.0014	0.0029	0.0012	0.0026	0.0026		0.0033	
	\bar{U}	0.0037 (2)	0.0034	0.0022	0.0037	0.0021	0.0034	0.0034		0.0037	
x	$U_z - \bar{U}$	-0.0007 (4)	-0.0008	-0.0008	-0.0008	-0.0009	-0.0008	-0.0008		-0.0004	
	$\frac{1}{2}(U_{\parallel} - U_{\perp}) = -U_{12}$	0.0005 (2)	0.0005	0.0004	0.0005	0.0004	0.0005	0.0005		0.0010	
	x	0.3031 (2)	0.3030 (2)	0.3030 (2)	0.3031 (2)	0.3030 (2)	0.3030 (2)	0.3030 (2)			

Secondly, we list the mean isotropic square amplitude $\bar{U} = \frac{1}{3}(U_x + U_y + U_z) = \frac{1}{3}(U_{11} + U_{22} + U_{33})$.

The 'prolateness' of the thermal motion $\Delta_1 U$ is equal to $U_z - \bar{U}$ and the 'non-axiality' $\Delta_2 U$ is $\frac{1}{2}(U_x - U_y) = -U_{12}$.

They refer to the spherical harmonic representation $(U_x S_x^2 + U_y S_y^2 + U_z S_z^2) = S^2[\bar{U} + \Delta_1 U \frac{1}{2}(3 \cos^2 \theta_s - 1) + \Delta_2 U \frac{1}{2} \sin^2 \theta_s \cos^2 2\varphi_s]$ where S , θ_s , φ_s are the spherical coordinates of the scattering vector, cf. Kurki-Suonio (1977). The values of model (1) are regarded as the numerical results of our work. The errors given are, rather arbitrarily, $\delta = (\delta_1^2 + \delta_2^2)^{1/2}$ where δ_1 is the statistical error given by the computer program and δ_2 is the range variation due to variations of the model [neglecting the discarded model (2)] divided by 3.4 (corresponding to the σ value of an even distribution over the range). For comparison, the experimental values of Niederauer & Gottlicher (1970) and Baur & Khan (1971) are added.

The anisotropy parameters $\Delta_1 U$ and $\Delta_2 U$ are much more independent of the model and, hence, more reliable than the average or isotropic \bar{U} . In particular, the room-temperature value $\Delta_2 U$ for fluorine, indicating a large anisotropy of motion in the xy plane, is well determined by our data. The other values of $\Delta_2 U$ are consistently very small for all models, and the corresponding anisotropies are almost insignificant, at least for Mg^{2+} at 52 K. The negative values of $\Delta_1 U$ are also independent of the model and indicate oblateness of the thermal motion with respect to the tetragonal axis. The

effect is clearly larger at room temperature and for F^- , and insignificant only for Mg^{2+} at 52 K.

The isotropic mean-square amplitudes show the greatest variations with the model. However, the main discrepancy ($\sim 30\%$) comes from the models allowing only particle-size extinction. Discarding these we are left with variations of the order of 10%.

Further, we can note that the mean-square amplitude U_{\perp} of the vibration perpendicular to the bond in the xy plane at room temperature for F^- is twice that for Mg^{2+} , while U_{\parallel} is the same for both. This corresponds to a concrete picture with the linear MgF_2 molecule vibrating almost rigidly in the xy plane. This is remarkably different from the situation at 52 K where both ions vibrate almost isotropically, with their different amplitudes.

This picture is in accordance with the lattice-dynamical considerations of Almairac & Benoit (1974) which show that the libration-like transverse optical mode of type B_{1g} or F_3^- has a low frequency at $K = 0$. Their measurements by inelastic neutron scattering give a value of 2.68 THz consistent with the Raman scattering result 2.76 THz of Porto, Fleury & Damen (1967). This corresponds to an excitation temperature of about 130 K which means that this mode will be strongly excited at 300 K but not at 52 K. Recent lattice-dynamical calculations based on the Almairac & Benoit (1974) model and performed by Galtier (1978) shown in the last column of Table 9 compare favourably with our experimental results and confirm our

preference for model (1). The greatly simplified Debye model calculation of Sirdeshmukh & Rao (1971) at room temperature cannot be valid, because the strong excitation of the soft optical mode destroys the validity of the Debye model.

The earlier X-ray diffraction results of Niederauer & Gottlicher (1970) and Baur & Khan (1971) at room temperature shown in Table 9 for comparison give clearly larger values for the mean isotropic temperature factors. In the former work no anisotropy was observed while the anisotropy parameters $\Delta_1 U$ and $\Delta_2 U$ obtained from the latter are in fair agreement with ours.

The results obtained lend themselves to use in charge-density analysis on the basis of X-ray data. The reliability of the bond length and the anisotropy parameters will make possible a more detailed interpretation of the anisotropic features of the atomic-charge distributions independent of the uncertainty of the spherical information. Lattice-dynamical calculations and more reliable means to evaluate or remove the effect of extinction would be necessary for more accurate spherical information on the ions.

The authors GV-V and J-PV would like to thank the Institut Laue-Langevin for making the neutron measurements possible and for technical assistance and financial support. They are indebted to Professor E. F. Bertaut for his continued interest in this subject.

References

- ALEKSANDROV, K. S., SHABANOVA, L. A. & ZINENKO, V. I. (1969). *Phys. Status Solidi*, **33**, 1–3.
- ALMAIRAC, R. & BENOIT, C. (1974). *J. Phys. Chem.* **7**, 2614–2648.
- BACON, G. E. (1977). *Neutron Diffraction Newsletter*, May 1.
- BAUR, W. H. & KHAN, A. A. (1971). *Acta Cryst.* **B27**, 2133–2139.
- BECKER, P. J. & COPPENS, P. (1975). *Acta Cryst.* **A31**, 417–425.
- COPPENS, P. & HAMILTON, W. C. (1970). *Acta Cryst.* **A26**, 71–83.
- GALTIER, M. (1978). Private communication.
- International Tables for X-ray Crystallography* (1969). Vol. I. Birmingham: Kynoch Press.
- KURKI-SUONIO, K. (1967). *Ann. Acad. Sci. Fenn. Ser. A6*, 263.
- KURKI-SUONIO, K. (1977). *Isr. J. Chem.* **16**, 115–123; 132–136.
- LEHMANN, M. & LARSEN, F. K. (1974). *Acta Cryst.* **A30**, 580–584.
- NIEDERAUER, K. & GOTTLICHER, S. (1970). *Z. Angew. Phys.* pp. 16–21.
- PORTO, S. P. S., FLEURY, P. A. & DAMEN, T. C. (1967). *Phys. Rev.* **154**, 522–526.
- SCHNEIDER, J. R. (1974). *J. Appl. Cryst.* **7**, 541–554.
- SIRDESHMUKH, D. B. & RAO, M. J. M. (1971). *Phys. Status Solidi B*, **44**, 105–106.
- THORNLEY, F. R. & NELMES, R. J. (1974). *Acta Cryst.* **A30**, 748–757.
- VIDAL-VALAT, G. (1975). Thèse d'Etat Montpellier CNRS AO No. 11914.
- WERNER, S. A. (1971). *Acta Cryst.* **A27**, 665–669.
- WITH, G. DE, HARKEMA, S. & FEILS, D. (1976). *Acta Cryst.* **B32**, 3178–3184.

Acta Cryst. (1979). **B35**, 1590–1593

Die Kristallstruktur von Barium Titanat $\text{Ba}_2\text{Ti}_{3,5}\text{O}_{13}$

VON WOLFGANG HOFMEISTER UND EKKEHART TILLMANN

Institut für Geowissenschaften, Postfach 3980, D-6500 Mainz, Bundesrepublik Deutschland

(Eingegangen am 26. Januar 1979; angenommen am 10. April 1979)

Abstract

Barium titanate $\text{Ba}_2\text{Ti}_{3,5}\text{O}_{13}$, monoclinic, $C2/m$ with $a = 15.160$ (4), $b = 3.893$ (1), $c = 9.093$ (2) Å, $\beta = 98.6$ (1)°, $Z = 2$, $D_x = 4.670$ Mg m⁻³. The crystal structure was determined from Patterson and Fourier syntheses and refined to $R = 0.034$ for 1563 observed reflections. The Ti atoms have distorted octahedral coordination with an average Ti–O distance of 2.00 Å; the Ba atoms are coordinated by 11 O atoms (average

Ba–O distance: 2.93 Å). $\text{Ba}_2\text{Ti}_{3,5}\text{O}_{13}$ is isostructural with $\text{Na}_2\text{Ti}_6\text{O}_{13}$, $\text{K}_2\text{Ti}_6\text{O}_{13}$ and $\text{Rb}_2\text{Ti}_6\text{O}_{13}$ with one of the three different Ti positions only partly occupied.

Einleitung

Farblose Einkristalle von $\text{Ba}_2\text{Ti}_{3,5}\text{O}_{13}$ wurden von Negas, Roth, Parker & Minor (1974) durch teilweises Aufschmelzen einer Probe der Zusammensetzung